Cancer Therapy: Preclinical

Clinical Cancer Research

PLK1 Inhibitors Synergistically Potentiate HDAC Inhibitor Lethality in Imatinib Mesylate–Sensitive or –Resistant BCR/ABL$^+$ Leukemia Cells *In Vitro* and *In Vivo*

Girija Dasmahapatra[1], Hiral Patel[1], Tri Nguyen[1], Elisa Attkisson[1], and Steven Grant[1,2,3]

Abstract

Purpose: To determine whether Polo-like kinase 1 (PLK1) inhibitors (e.g., BI2536) and histone deacetylase (HDAC) inhibitors (e.g., vorinostat) interact synergistically in the BCR/ABL$^+$ leukemia cells sensitive or resistant to imatinib mesylate (IM) *in vitro* and *in vivo*.

Experimental Design: K562 and LAMA84 cells sensitive or resistant to imatinib mesylate and primary CML cells were exposed to BI2536 and vorinostat. Effects on cell viability and signaling pathways were determined using flow cytometry, Western blotting, and gene transfection. K562 and BV173/E255K animal models were used to test *in vivo* efficacy.

Results: Cotreatment with BI2536 and vorinostat synergistically induced cell death in parental or imatinib mesylate–resistant BCR/ABL$^+$ cells and primary CD34$^+$ bone marrow cells but was minimally toxic to normal cells. BI2536/vorinostat cotreatment triggered pronounced mitochondrial dysfunction, inhibition of p-BCR/ABL, caspase activation, PARP cleavage, reactive oxygen species (ROS) generation, and DNA damage (manifest by increased expression of γH2A.X, p-ATM, p-ATR), events attenuated by the antioxidant TBAP. PLK1 short hairpin RNA (shRNA) knockdown significantly increased HDACI lethality, whereas HDAC1–3 shRNA knockdown reciprocally increased BI2536-induced apoptosis. Genetic interruption of the DNA damage linker H1.2 partially but significantly reduced PLK1/HDAC inhibitor–mediated cell death, suggesting a functional role for DNA damage in lethality. Finally, BI2536/vorinostat cotreatment dramatically reduced tumor growth in both subcutaneous and systemic BCR/ABL$^+$ leukemia xenograft models and significantly enhanced animal survival.

Conclusions: These findings suggest that concomitant PLK1 and HDAC inhibition is active against imatinib mesylate–sensitive or refractory CML and ALL cells both *in vitro* and *in vivo* and that this strategy warrants further evaluation in the setting of BCR/ABL$^+$ leukemias. *Clin Cancer Res; 19(2); 404–14. ©2012 AACR.*

Introduction

Chronic myelogenous leukemia (CML) is neoplastic stem cell disorder characterized by the 9,22 translocation, producing the BCR/ABL fusion protein, a constitutively active kinase which signals downstream to multiple anti-apoptotic proteins (e.g., CRKL, STAT5, and Bcl-xL; ref. 1). CML treatment has been revolutionized by the BCR/ABL kinase inhibitor imatinib mesylate (IM) and second-generation agents (e.g., nilotinib, dasatinib, and bosutinib; refs. 2, 3). Despite long-term responses to these agents, drug intolerance, the development of resistance-conferring mutations (e.g., T315I), and the failure to eradicate primitive leukemia-initiating cells represent therapeutic challenges (4). In addition, patients in blast phase of CML or with Ph^{1+} acute lymphoblastic leukemia (ALL) generally respond poorly to therapy (5). Consequently, the need for new and more effective treatment options remains.

Polo-like kinase 1 (PLK1) is a conserved serine-threonine kinase involved in mitotic progression through interactions with cyclin B, the CDC25C phosphatase, and Wee1 (6). It has been implicated in progression into M phase, mitotic spindle formation, cytokinesis, and chromosome segregation (7). PLK1 modulates DNA damage responses, including recovery from the G_2 DNA damage checkpoint (8). Moreover, interactions between PLK1 and multiple checkpoint proteins, including Chk1/2, p53, claspin, and FoxM1, have been described (9). PLK1 is highly expressed in

Authors' Affiliations: [1]Division of Hematology/Oncology, Department of Medicine, Virginia Commonwealth University, [2]the Massey Cancer Center, and [3]Virginia Institute of Molecular Medicine, Virginia Commonwealth University, Richmond, Virginia

Note: Supplementary data for this article are available at Clinical Cancer Research Online (http://clincancerres.aacrjournals.org/).

Corresponding Author: Steven Grant, 234 Goodwin Research Laboratory, Massey Cancer Center, MCV/VCU, 401, College Street, Richmond, VA 23298. Phone: 804-828-5211; Fax: 804-828-2174; E-mail: stgrant@vcu.edu

doi: 10.1158/1078-0432.CCR-12-2799

Translational Relevance

The introduction of BCR/ABL kinase inhibitors, such as imatinib or dasatinib, resulted in improved treatment for patients with chronic myelogenous leukemia (CML) but many become refractory through various mechanisms, including mutations in kinase domain. Consequently, novel strategies are urgently needed to this disease. Recent evidence that Polo-like kinase 1 (PLK1) acts downstream of BCR/ABL makes it an attractive target for CML therapy, as it may be capable of circumventing resistance to BCR/ABL kinase inhibitors. The present findings indicate that histone deacetylase (HDAC) inhibitors, such as vorinostat, interact synergistically with a clinically relevant PLK1 inhibitor (BI2536) in imatinib mesylate–resistant cells both *in vitro* and *in vivo* through multiple mechanisms, raising the possibility that a combined HDAC/PLK1 inhibitor strategy may be of value in patients with CMLs resistant to standard approaches.

multiple malignancies, including leukemia (10) and lymphoma (11), prompting the development of multiple PLK1 inhibitors, including the specific ATP-competitive inhibitor BI2536, which displays a 10,000-fold increase (12) in specificity for PLK1 compared with other tyrosine and threonine kinases (12). It was recently reported that PLK1 represented a downstream target of BCR/ABL in CML cells and that PLK1 interruption by inhibitors such as BI2536 or short hairpin RNA (shRNA) knockdown promoted leukemia cell death in highly imatinib mesylate–resistant cells expressing BCR/ABL gatekeeper mutations (e.g., T315I; ref. 13). BI6727 (volasertib) is a highly potent, clinically relevant PLK1 inhibitor which has superior pharmacokinetic properties compared with BI2536 (14).

Histone deacetylase inhibitors (HDACI) act by modifying chromatin structure and, by extension, gene expression (15). These agents also trigger acetylation of various nonhistone proteins, particularly those implicated in DNA damage responses, including DNA repair proteins (Ku70) and chaperone proteins (Hsp90; ref. 16). In addition, HDACIs downregulate DNA repair proteins (e.g., Rad51 and MRE11; refs. 17). Indeed, HDACI lethality has been attributed to oxidative injury [e.g., reactive oxygen species (ROS); ref. 18], due to impaired induction of antioxidant proteins (19). HDACIs have been shown to enhance the activity of tyrosine kinase inhibitors in CML cells (20), including early progenitor cells (21). Currently, no information exists concerning PLK1/HDACI interactions in human CML cells. Consequently, interplay between BI2536 and the HDACI vorinostat has been examined in BCR/ABL$^+$ leukemia cells (both CML and ALL), including highly imatinib mesylate–resistant cells expressing gatekeeper mutations. The present results show highly synergistic interactions both *in vitro* and *in vivo* in imatinib mesylate–sensitive and -resistant BCR/ABL$^+$ leukemia cells and suggest multiple mechanisms, including enhanced inhibition of BCR/ABL and downstream targets, as well as marked potentiation of oxidative injury and DNA damage. These findings provide a theoretical foundation for a strategy combining HDAC and PLK1 inhibitors to eradicate BCR/ABL$^+$ leukemia cells.

Materials and Methods

Cells

LAMA 84 cells were purchased from the German Collection of Microorganisms and Cell Cultures. K562 and BaF/3 cells were obtained as before (22). Cells were cultured in RPMI media as described previously (22). CD34$^+$ cells were obtained with informed consent from patient bone marrows and processed as before (22). CML adult T315I and BV173/E255K ALL cells were generated as described (23). K562 cells expressing ectopically PLK1-CA or shRNA/scrambled sequence were generated by electroporation (Amaxa) as described (24). K562 and LAMA84 cell lines were authenticated by STR DNA fingerprinting using the AmpFlSTR Identifiler Kit (Applied Biosystems). The short tandem repeat (STR) profiles were compared with known American Type Culture Collection database and to the German Collection of Microorganisms and Cell Cultures database (http://www.dsmz.de/).

Reagents

PLK1 inhibitors BI2536 and BI6277 were purchased from ChemieTek Inc. and Selleck BioChem. GW843682 and 7-aminoactinomycin D (7-AAD) were from Sigma-Aldrich and vorinostat was from Merck. All drugs were formulated in sterile dimethyl sulfoxide (DMSO) before use. Annexin V/propidium iodide (PI) was from BD PharMingen and MnTBAP was from Calbiochem.

Assessment of cell viability and apoptosis

Cell viability was monitored by flow cytometry using 7-AAD as before (24). Apoptosis was evaluated by Annexin V/PI staining (24) and verified by Wright–Giemsa staining. Results of morphologic assessment, 7-AAD staining, and Annexin V/PI staining were highly concordant.

Separation of S-100 fractions and assessment of cytochrome *c* release

Cells were harvested and cytosolic S-100 fractions were prepared as before (22, 24). Western blot analysis assessing cytochrome *c*, SMAC, and AIF release was conducted as below.

Immunoblot analysis

Immunoblotting was conducted as described previously (22, 24). Primary antibodies were as follows: AIF, cytochrome *c*, p-stat5, stat5, p-ATM, and ATR (Santa Cruz Biotechnology); p-BCR/ABL, BCR/ABL, p-PLK1(Thr210), PLK1, cleaved caspase-3, and p-ATR (Cell Signaling Technology); PARP (C-2–10; BioMol Research Laboratories); SMAC and γH2A.X (Upstate Biotechnology); tubulin (Oncogene); ATM and Histone1.2 (Abcam); and p-PLK1 (Ser137; Millipore).

Measurement of ROS production

Cells were treated with 20 μmol/L 2′,7′-dicholorodihydrofluorescein diacetate for 30 minutes at 37°C, and fluorescence was monitored by flow cytometry and analyzed with CellQuest software (25).

Cell-cycle analysis

Cell-cycle distribution was determined by flow cytometry using a commercial software program (ModFit, Becton Dickinson) as per standard protocol (25).

Plasmids and shRNA

Plasmids encoding *Homo sapiens* PLK1 in pCMV6-Entry vectors were obtained from Origene Technologies. Four separate sequences were used to knock down PLK1 (i.e., 1-GGCAAGATTGTGCCTAAGTCTCTGCTGCT, 2-ACCAGCACGTCGTAGGATTCCACGGCTT, 3-TCACAGTCCTCAATAAAGGCTTGGAGAAC, 4- TGGACTGGCAACCAAAGTCGAATATGACG) and one nonspecific control sequence (NC-GGAATCTCATTCGATGCATAC) as negative control. Similarly, the following sequences are used to known down Histone 1.2 (AAGGTTGCGAAGCCCAAGAAA, NC- GGAATCTCATTCGATGCATAC from SA Biosciences). Details of the shRNA for knocking down HDAC1–3 are follows (shHDAC1: 5′-GCTCCATCCGTCCAGATAACA-3′; shHDAC2: 5′-GCTGGAGCTGTGAAGTTAAAC3-′; shHDAC3: 5′-GCACCATGCCAAGAAGTTTGA-3′; NC- GGAATCTCATTCGATG CATAC).

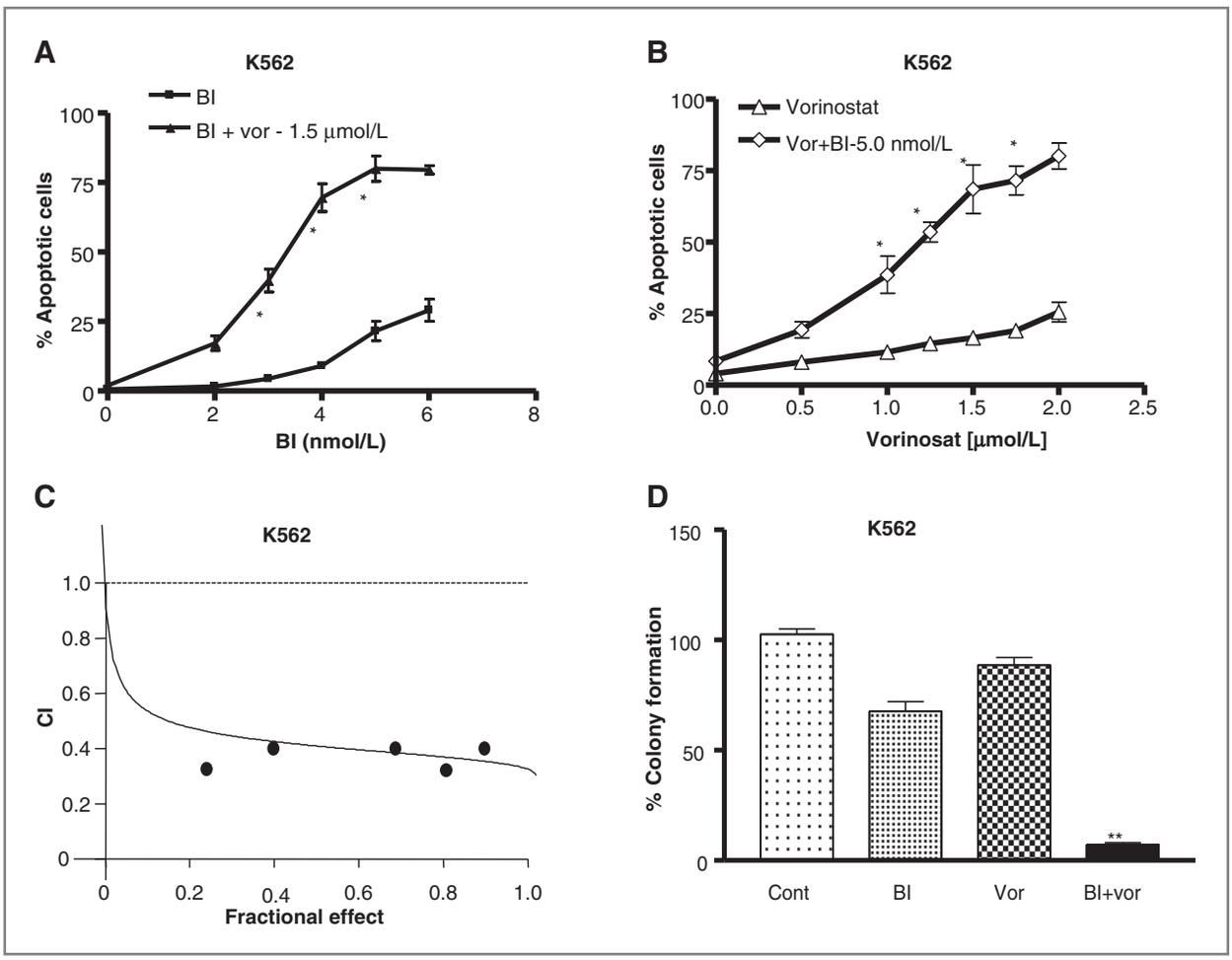

Figure 1. Cotreatment with BI2536 and vorinostat synergistically induces cell death and dramatically reduces colony formation in K562 cell (A). K562 cells were treated with either BI2536 (1.0–6.0 nmol/L) or in combination with fixed vorinostat (1.5 μmol/L) concentrations for 48 hours. B, K562 cells were treated with vorinostat (0.5–2.0 μmol/L) in the presence or absence of fixed concentrations of BI2536 (5.0 nmol/L) for 48 hours. C, fractional effect (FA) values were determined by comparing results obtained for untreated controls and treated cells following exposure to agents administered at a fixed ratio (BI: vor = 1:300), after which median dose–effect analysis was used to characterize the nature of the interaction. Combination index (CI) values less than 1.0 denote a synergistic interaction. D, K562 cells were treated with BI2536 (5 nmol/L) ± vorinostat (1.5 μmol/L) for 48 hours, after which cells were washed and plated in soft agar as described (23). Colonies, consisting of groups ≥ 50 cells, were scored at day 10. Values for each condition were expressed as a percentage of control colony formation. In all cases, values correspond to the means for triplicate determinations ± SD. A and B, *, significantly more than values for cells exposed to either BI2536 or vorinostat alone; $P < 0.02$; D, **, significantly less than values for cells exposed to either BI2536 or vorinostat alone; $P < 0.01$. For all studies, values represent the means for 3 experiments carried out in triplicate ± SD.

Transient transfections

Transient transfections of K562 cells used an Amaxa Nucleofector. Protocols for each cell line used Transfection Kit V and a cell-specific optimized protocol (T-16) as before (22).

Animal studies

Animal studies used Beige-nude-XID mice (NIH-III; Charles River). A total of 10×10^6 K562 cells were pelleted, washed twice with $1 \times$ PBS, and injected subcutaneously into the right flank. Once tumors were visible, 5 to 6 mice were treated with BI2536 with or without vorinostat and tumor growth or regression monitored as before (24, 25). To investigate effects of tumor size on regimen efficacy, experiments were carried out with different initial tumor sizes [e.g., (i) average, 150 mm^3 and (ii) average, 550 mm^3. Systemic tumor models used BV173/E255K/Luc cl4 cells as described earlier (23). Briefly, 2×10^6 BV173/E255K/Luc cl4 cells in 100 μL PBS were tail vein injected and animals noninvasively imaged using an *in vivo* Imaging System (IVIS-200; Xenogen) following luciferase injection (D-luciferin; Research Products International). BI2536 was administered orally by gavage; vorinostat was given intraperitoneally. Both drugs were given simultaneously daily, 3 days a week (TIW). BI2536 was dissolved in 0.1 (N) HCl solution; 0.9% NaCl was added as diluent. The BI2536 volume was 100 μL. Vorinostat was administered as described (24).

Statistical analysis

The significance of differences between experimental conditions was determined with the 2-tailed Student *t* test. Synergistic and antagonistic interactions were characterized using median dose–effect analysis in conjunction with a commercially available software program (CalcuSyn; ref. 26).

Results

HDACIs dramatically increase PLK1 lethality toward IM-sensitive or -resistant BCR/ABL$^+$ leukemia cells but not normal CD34$^+$ cells

Concomitant exposure (48 hours) of K562 cells to vorinostat (1.5 μmol/L) and very low, minimally toxic (e.g., 3 nmol/L) concentrations of BI, significantly increased apoptosis, which exceeded 80% at 5 to 6 nmol/L BI2536 (Fig. 1A). Vorinostat concentrations as low as 0.5 μmol/L, potentiated BI lethality which became more pronounced at concentrations $\geq$ 1.0 μmol/L (Fig. 1B). Time course analysis revealed discernible increases in cell death after 24 hours of exposure, which increased at 48 hours (Supplementary Fig. S1A). Median dose–effect analysis yielded combination

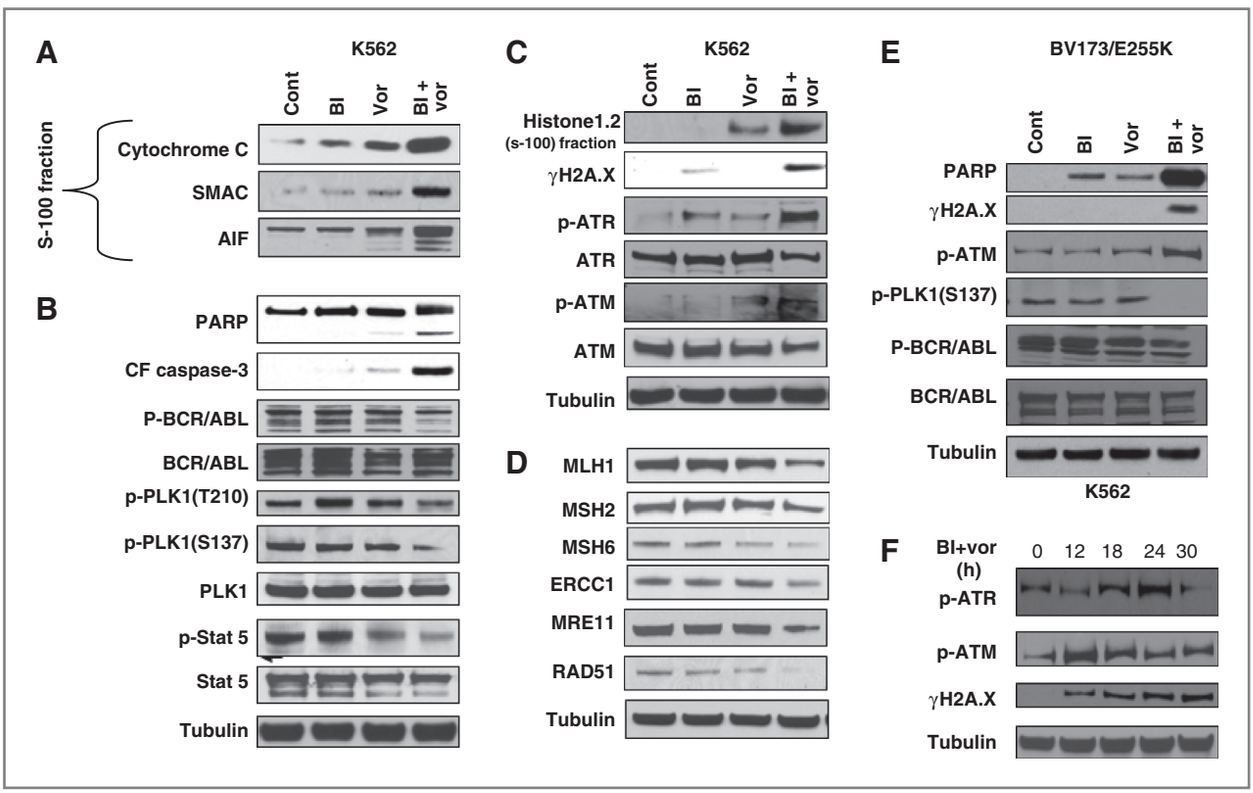

Figure 2. Co-exposure of parental K562 or imatinib-resistant BV173/E255 cells to BI2536 and vorinostat leads to modulation of BCR/ABL and stress-related pathways. K562 cells were treated with BI2536 (5.0 nmol/L) ± vorinostat (1.5 μmol/L; A–D) for 24 hours. E, BV173/E255 cells were treated (24 hours) with BI2536 (3.0 nmol/L) ± vorinostat (0.75 μmol/L). F, K562 cells were treated with BI2536 (5.0 nmol/L) ± vorinostat (1.5 μmol/L) for the designated intervals. Expression of the indicated proteins was determined by Western blotting using the indicated antibodies. Each lane was loaded with 20 μg of protein; blots were stripped and reprobed with antibodies to tubulin to ensure equivalent loading and transfer. Results are representative of 3 independent experiments.

index values considerably below 1.0, reflecting a highly synergistic interaction (Fig. 1C). Combined treatment also strikingly reduced colony formation of K562 cells (Fig. 1D). In contrast, individual or combined treatment with BI and vorinostat minimally affected normal $CD34^+$ cells (Supplementary Fig. S1B).

Similar interactions were observed when BCR/ABL^+ LAMA84 were exposed to BI (2.0 nmol/L) and 1.0 μmol/L vorinostat (Supplementary Fig. S2A) or in K562 cells exposed to other PLK1 inhibitors (e.g., BI6277 or GW843682) or HDACIs (e.g., vorinostat or SBHA; Supplementary Fig. S2B). Median dose–effect analysis revealed synergism between GW843682 and vorinostat in LAMA84 cells (Supplementary Fig. S2C). Notably, BI2536/vorinostat synergism occurred in highly imatinib mesylate–resistant human T315I BCR/ABL^+ ALL cells or E255K BV173 ALL cells bearing the E255K mutation (ref. 23; Supplementary Fig. S2D and S2E). In contrast to normal $CD34^+$ cells, BI2536/vorinostat induced marked apoptosis in primary BCR/ABL^+ $CD34^+$ cells (Supplementary Fig. S2F). Finally, the BI2536/vorinostat regimen exerted pronounced lethality toward BaF/3 cells expressing wild-type (wt) or 3 BCR/ABL mutants (E255K, M351T, or T315I; Supplementary Fig. S2G). In separate studies, sequential administration of BI2536 and vorinostat was slightly less effective than simultaneous exposure in inducing cell death (data not shown). These findings indicate that HDACIs synergistically potentiate the lethality of extremely low concentrations of PLK1 inhibitors in imatinib mesylate–sensitive or -resistant BCR/ABL^+ leukemia cells but are relatively sparing toward their normal counterparts.

HDACI/BI2536 co-administration enhances BCR/ABL inhibition and DNA damage

Effects of vorinostat/BI2536 on various signaling and survival events were examined. These studies were conducted at relatively early exposure intervals and before the onset of extensive apoptosis (e.g., 24 hours). Combined treatment of K562 cells with BI2536 (5 nmol/L) and vorinostat (1.5 μmol/L) resulted in a marked increase in cytochrome *c*, AIF, and SMAC release into the cytosolic fraction, accompanied by enhanced PARP and caspase-3 cleavage (Fig. 2A and B). While the agents administered alone had little effect on BCR/ABL phosphorylation, combined treatment induced modest reductions in phospho-BCR/ABL expression but not total expression (Fig. 2B). Combined treatment had little effect on T210 phosphorylation of PLK1 but clearly reduced S137 phospho-PLK1. No changes in total PLK1 were noted. Finally, combined treatment reduced levels of phospho-STAT5, a downstream BCR/ABL target (27).

While vorinostat alone modestly upregulated histone 1.2, a marker of DNA damage (28), co-administration of BI-2536, which had no effect by itself, dramatically increased histone 1.2 levels, accompanied by pronounced induction

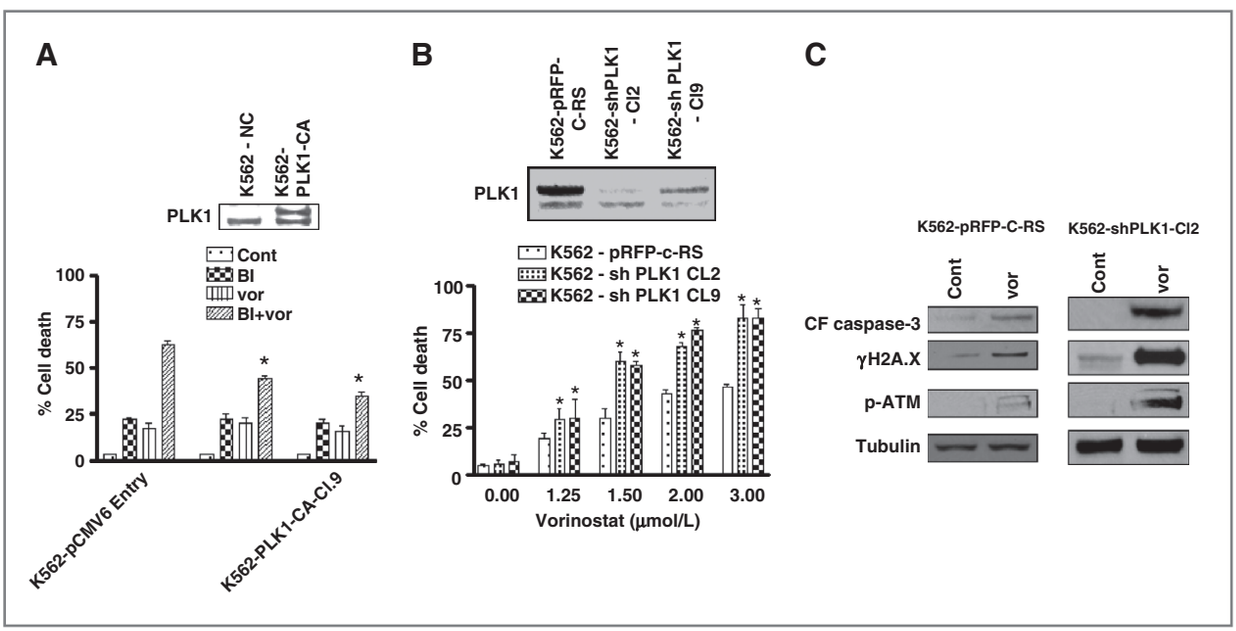

Figure 3. PLK1 protein expression plays a significant functional role to potentiate the lethality of vorinostat in K562 cells. K562 cells were stably transfected with (A) PLK1-CA or empty vector (pCMV6-Entry) cDNA (Inset: Western blot analyses showing expression of PLK1 expression in empty vector control and overexpressing cells) and exposed (48 hours) to BI2536 (6.0 nmol/L) ± vorinostat (1.25 μmol/L). B, shPLK1 or empty vector control pRFP-C-RS cDNA and exposed (48 hours) to indicated concentration of vorinostat, after which cell death was monitored by 7-AAD staining and flow cytometry (Inset: Western blot analyses showing expression of PLK1 expression in empty vector control and knockdown cells). Results represent the means ± SD for 3 separate experiments carried out in triplicate. C, K562 cells expressing either shPLK1 or empty vector control pRFP-C-RS cDNA as (B) above and treated with vorinostat (1.5 μmol/L) for 24 hours, after which Western blot analysis was conducted to monitor expression of the indicated proteins. For A and B, *, significantly greater than values obtained for empty vector controls; $P < 0.05$.

of γH2A.X, an indicator of DNA double-strand breaks (ref. 29; Fig. 2C). Combined treatment also resulted in clear increases in phosphorylation of the checkpoint proteins ATR and ATM (Fig. 2C), accompanied by downregulation of DNA repair proteins (e.g., MLH1, MSH3, MSH6, MRE11, and RAD51; Fig. 2D). Increased DNA damage occurred in highly imatinib mesylate–resistant BV173/E255 ALL cells (Fig. 2E). Finally, time course studies of K562 cells exposed to BI2536 and vorinostat resulted in clear increases in γH2A.X formation and ATM phosphorylation at 12 hours and ATR phosphorylation at 18 hours (Fig. 2F). In separate studies, co-administration of the broad caspase inhibitor BOC-FMK did not prevent DNA damage or ATM/ATR phosphorylation by the BI2536/vorinostat regimen (data not shown). Finally, histone 1.2 knockdown significantly reduced BI2536/vorinostat lethality ($P < 0.05$; Supplementary Fig. S3A) and diminished PARP cleavage (Supplementary Fig. S3B). Collectively, these findings indicate that the BI2536/vorinostat regimen downregulates various survival proteins and promotes DNA damage in BCR/ABL$^+$ leukemia cells and argue for a functional role for DNA damage in lethality.

PLK1 depletion increases HDACI lethality in BCR/ABL$^+$ cells

To evaluate the functional significance of PLK1 in these interactions, K562 cells ectopically expressing PLK1 were generated. Two clones (CA6 and CA9) expressing significantly greater levels of PLK1 than scrambled controls (Fig. 3A, inset) were used. The lethality of the BI2536 regimen in PLK1-expressing clones was significantly attenuated ($P < 0.05$) compared with controls (Fig. 3A). Conversely, shRNA knockdown of PLK1 (Fig. 3B, inset) significantly increased vorinostat lethality (Fig. 3B). Finally, PLK1-knockdown cells exposed to vorinostat exhibited significant increases in caspase-3 cleavage, γH2A.X formation, and ATM phosphorylation compared with controls (Fig. 3C).

ROS generation by the BI2536/vorinostat regimen plays a significant functional role in lethality

Previous evidence implicated oxidative injury in HDACI lethality toward myeloid leukemia cells (18, 30). While BI2536 and vorinostat alone modestly induced ROS, manifested as early as 30 minutes after administration and increasing over the ensuing 24 hours, combined treatment significantly increased ROS levels (Fig. 4A). Notably, the ROS scavenger TBAP blocked ROS generation (Fig. 4B) as well as lethality (Fig. 4C) in BI2536/vorinostat-treated cells. TBAP also blocked BI2536/vorinostat-mediated caspase-3 and PARP cleavage, γH2A.X formation, and ATM/ATR phosphorylation (Fig. 4D), suggesting a functional role for oxidative injury in DNA damage and lethality.

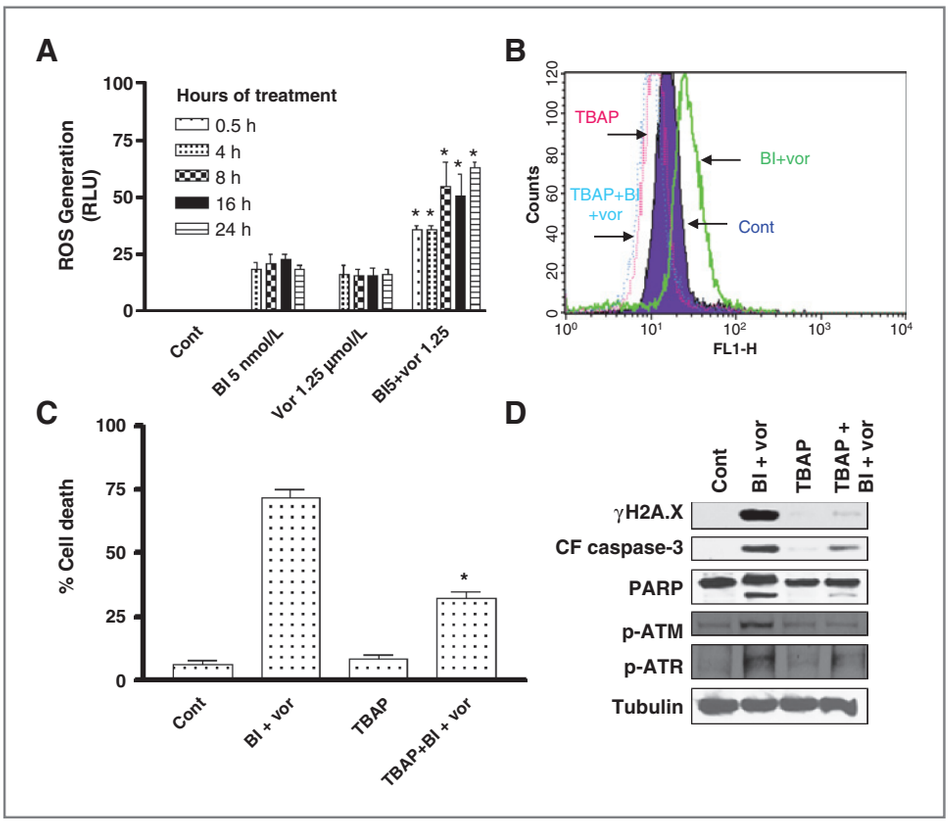

Figure 4. Combined BI2536/vorinostat treatment robustly induces ROS generation which is circumvented by antioxidants. A, K562 cells were treated with BI2536 (5.0 nmol/L) ± vorinostat (1.5 μmol/L) after which ROS generation was monitored at the indicated intervals. B, K562 cells were treated with BI2536 (5.0 nmol/L) ± vorinostat (1.5 μmol/L) ± pretreatment (3 hours) with 400 μmol/L TBAP for 24 hours, after which ROS generation was monitored as described in Materials and Methods. C, after treatment of K562 cells as in (B) for 48 hours, cell death was monitored by 7-AAD staining. D, following 24 hours of drug exposure as in (C) above, expression of the indicated proteins was monitored by Western blotting. Blots were stripped and reprobed with anti-tubulin antibodies to ensure equal loading and transfer of protein (20 μg each lane). For A, *, significantly different from values for single drug treatment; C, *, significantly different from values for combination treatment without TBAP pretreatment controls; $P < 0.05$.

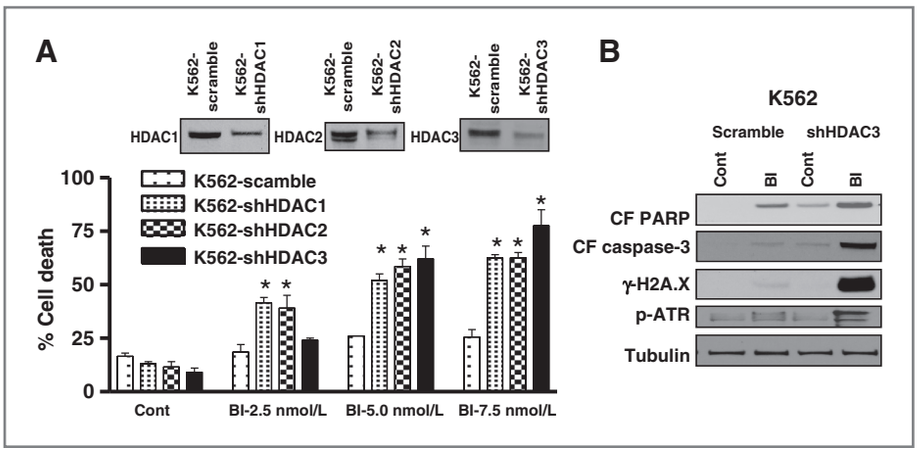

Figure 5. Knocking down of HDAC1–3 by shRNA potentiates the lethality of BI2536 in K562 cell. A, K562 cells were transiently transfected with HDAC1–3 shRNA or scramble, respectively, and exposed (48 hour) to the indicated concentration of BI2536, after which cell death was monitored by 7-AAD staining and flow cytometry. Results represent the means ± SD for 3 separate experiments carried out in triplicate. Inset: Western blot analyses showing expression of HDACs expression in empty vector control and knockdown cells. B, cells were transfected with HDAC3 scrambled sequence or shRNA as described above in (A) and treated with BI2536 (5.0 nmol/L) for 24 hours, after which Western blot analysis was conducted to monitor expression of the indicated proteins. For A, *, significantly greater than values obtained for empty vector controls; $P < 0.05$.

HDAC knockdown increases BI-2536 lethality in BCR/ABL$^+$ leukemia cells

Previous studies have implicated HDACs (e.g., HDAC3) in the DNA damage response (31). Consequently, the effects of HDAC knockdown on responses to BI2536 were examined. Three transiently transfected lines exhibiting knockdown of HDAC1–3 respectively (Fig. 5A, inset) were significantly more susceptible to BI2536 lethality (2.5–7.5 nmol/L) than controls (Fig. 5A). Moreover, HDAC3 knockdown cells exposed to BI2536 displayed increased caspase-3 and PARP cleavage, λH2A.X formation, and phospho-ATR compared with controls (Fig. 5B). Similar results were obtained in HDAC1 or 2 knock-down cells (data not shown), arguing that interference with HDAC function contributes to BI2536/vorinostat anti-leukemic interactions.

Co-administration of BI2536 prevents vorinostat-induced G_1 arrest and promotes G_2–M accumulation

Exposure to vorinostat alone (24 hours) induced a marked increase in the G_1 fraction, consistent with previous reports (refs. 32, 33; Supplementary Fig. S4A). BI2536 by itself modestly increased G_2–M accumulation and slightly reduced the G_1 fraction. However, vorinostat/BI2536 co-administration induced pronounced G_2–M accumulation, accompanied by an increase in the subdiploid (apoptotic) population (Supplementary Fig. S4A). Virtually identical changes were observed in PLK1 shRNA knockdown cells exposed to vorinostat but not in controls (Supplementary Fig. S4B and S4C), raising the possibility that abrogation of HDACI-mediated G_1 arrest and accumulation of cells in G_2–M may be due to enhanced DNA damage may contribute to BI2536/vorinostat lethality.

The BI2536/vorinostat regimen displays striking *in vivo* activity in early- and late-stage BCR/ABL$^+$ xenograft models

To assess the *in vivo* activity of the BI2536 regimen, 2 xenograft models were used. In the first, Beige mice were injected in the flank with 10×10^6 K562 cells; when tumors were first visible (volumes < 150 mm^3), animals were treated with BI2536 (30 mg/kg) ± vorinostat (70 mg/kg) for 2 weeks. Alternatively, identical treatment regimens were initiated when tumor volumes exceeded 550 mm^3. In the first model, vorinostat alone had little effect whereas BI2536 delayed but did not prevent tumor growth (Fig. 6A). However, combined treatment essentially abrogated tumors, which did not recur during the entire 38-day observation period. In the late-stage model, vorinostat alone had no effect, whereas BI2536 along marginally delayed tumor growth (Fig. 6B). However, combined treatment substantially reduced tumor size over the entire observation period. Western blot analysis of tumor sections obtained after 6 days of treatment (early-stage model) revealed that combined but not single-agent treatment downregulated phospho-BCR/ABL and downstream targets (phospho-STAT5 and -CRKL) while increasing PARP/caspase-3 cleavage and γH2A.X formation (Fig. 6C). Similar results were obtained in day-21 specimens (data not shown). Finally, BI2536 (30 mg/kg) and vorinostat (70 mg/kg) cotreatment significantly increased animal survival compared with no or single-agent treatment in a systemic imatinib-resistant luciferase-labeled BV173/E255K model ($P < 0.05$; Fig. 6D). Tumor weights for all treatment groups did not decline by more than 10%, and no other signs of toxicity (torpor, weight loss, etc.) were observed (data not shown).

The marked reduction in size of the flank tumors in BI2536/vorinostat-treated animals is shown in at the end

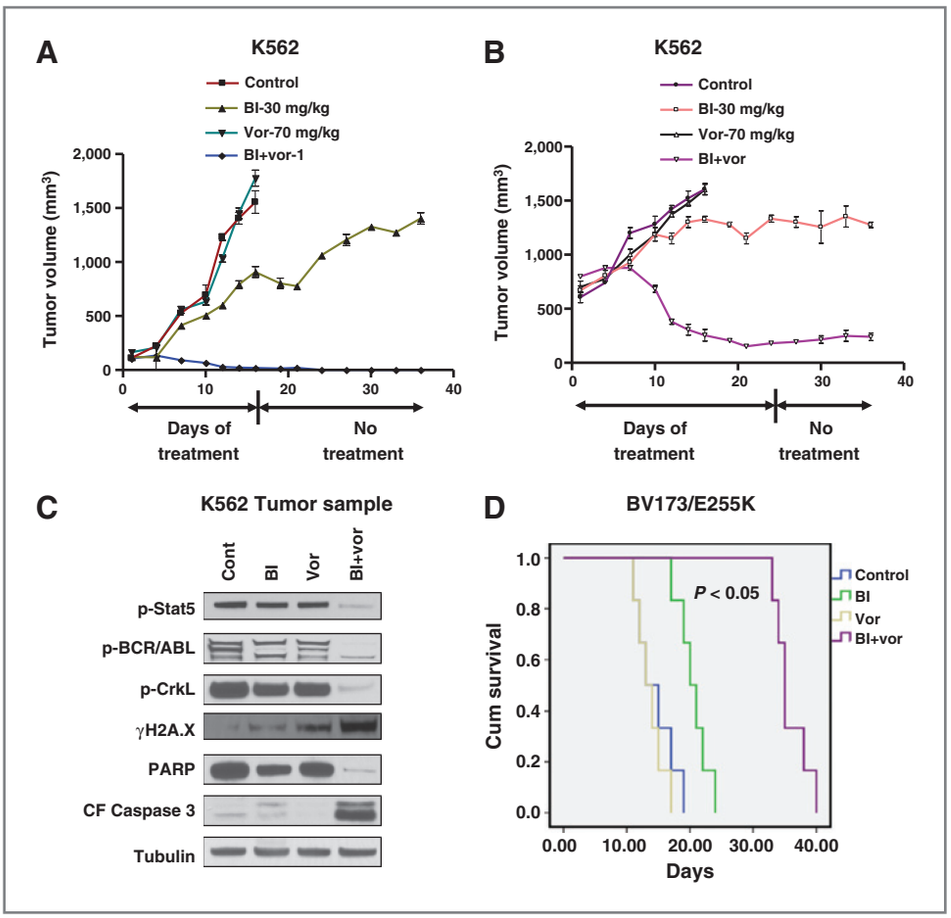

Figure 6. The BI2536/vorinostat regimen displays striking *in vivo* activity in BCR/ABL$^+$ xenograft models. Beige mice were injected in the flank with 10×10^6 K562 cells. Once tumors formed, mice were divided into 2 groups with average tumor sizes of approximately (A) 150 mm^3 or (B) 550 mm^3 and treated with the designated doses of BI2536 ± vorinostat thrice weekly as described in Materials and Methods for 14 or 24 days, respectively. Tumor volumes were measured twice weekly and mean tumor volumes were plotted against days of treatment. Tumor samples were extracted from mice after (C) 6 days (early-stage model) and of drug treatment and lysed with lysis buffer followed by sonication. Western blotting was conducted using the extracted proteins, which were probed with the indicated primary antibodies. Each lane was loaded with 20 μg of protein; blots were subsequently stripped and reprobed with antibodies to tubulin to ensure equivalent loading and transfer. D, survival curves of individual groups with systemically IM-resistant BV173/E255K tumors after 24 days following treatment with BI2536 (30 mg/kg) ± vorinostat (70 mg/kg) TIW. Control, blue; BI2536, green; vorinostat, yellow; BI2536 + vorinostat, purple, Survival was evaluated from the first day of treatment until death using Kaplan–Meier analysis (*, $P < 0.05$).

of drug treatment (Supplementary Fig. S5A) and 14 days after terminating the treatment (Supplementary Fig. S5B). Finally, combined treatment substantially reduced tumor growth compared with single-agent treatment in a systemic, luciferase-labeled BV173/E255K model system (Supplementary Fig. S5C). Collectively, these findings indicate that combined *in vivo* treatment with BI2536 and vorinostat induces many of events observed in *in vitro* studies and that this regimen exhibits pronounced *in vivo* activity against early- and late-stage leukemia xenograft models.

Discussion

The present results indicate that HDACIs strikingly increase PLK1 inhibitor (e.g., BI2536) lethality in BCR/ABL$^+$ leukemia cells, including those exhibiting marked resistance to imatinib mesylate through gatekeeper or other mutations. Previously, BI2536 showed single-agent activity against such cells and suggested that PLK1 represents an important BCR/ABL downstream target responsible for survival functions (13). Notably, HDACIs have been shown to enhance BCR/ABL kinase inhibitor activity through various mechanisms, including BCR/ABL downregulation due to chaperone function disruption (20, 34) or enhanced BCR/ABL inhibition (35). Here, vorinostat/BI2536 promoted modest inactivation/dephosphorylation of BCR/ABL and its downstream target STAT5 (27). The mechanism underlying HDACI/BI2536-mediated disruption of the BCR/ABL pathway remains to be determined, as does the contribution of BCR/ABL inhibition to lethality. Indeed, preliminary studies in BCR/ABL-negative acute myelogenous leukemia (AML) cells suggest similar PLK1/HDAC inhibitor interactions

(Dasmahapatra and Grant, unpublished observations). Such findings argue that BCR/ABL pathway inhibition is unlikely to be the sole mechanism of lethality for this regimen. Finally, vorinostat potentiated BI2536-mediated inhibition of PLK1 phosphorylation at Ser137, which has been implicated in late mitotic progression and the mitotic spindle checkpoint (36), potentially contributing to lethality.

The present results suggest that enhanced HDAC/PLK1 inhibitor lethality involves potentiation of DNA damage. HDACIs induce DNA damage through diverse mechanisms, including downregulation of DNA repair proteins (e.g., RAD51 and MRE11; ref. 17) or acetylation (e.g., Ku70; ref. 37). PLK1 also plays an important role in the mitotic spindle apparatus and DNA damage responses (38), suggesting that enhanced lethality stems from the disabling of the DNA damage and repair response. In support of this concept, combining BI2536 with vorinostat sharply increased expression of the atypical histone γH2A.X, reflecting double-strand DNA breaks (29) and DNA damage checkpoint kinase activation (ATM and ATR). Moreover, BI2536/vorinostat co-exposure produced reductions in the expression of multiple DNA repair proteins, including RAD51, MRE11, ERCC1, MSH2/6, and MLH1, compared with vorinostat alone. The mechanism underlying this phenomenon remains to be determined, but as in the case of BCR/ABL inactivation, may represent secondary, apoptosis-related events. In this context, knockdown of HDACIs (e.g., HDAC3) promotes DNA damage (31), possibly reflecting the contribution of HDACs to DNA repair complexes (39). Consistent with these findings, HDAC1–3 knockdown significantly increased BI2536-mediated DNA damage and lethality. Conversely, ectopic PLK1 expression significantly reduced BI2536/vorinostat-mediated apoptosis, whereas shRNA PLK1 knockdown significantly increased vorinostat-induced cell death, implicating on-target actions in synergistic interactions. Finally, the observation that knockdown of histone 1.2, which links DNA damage to the apoptotic apparatus (28) significantly protected cells, argues for a functional role for DNA damage in lethality.

HDACIs have been shown to kill transformed cells, including leukemia cells, through the induction of ROS (18), and selective induction of oxidative injury in transformed cells may reflect impairment in upregulation of antioxidant proteins (e.g., thioredoxin reductase; ref. 40). On the other hand, a link between PLK1 and oxidative injury has not previously been described. Interestingly, while minimally toxic vorinostat or BI2536 concentrations modestly induced ROS, combined treatment resulted in significant increases as early as 30 minutes after drug exposure which persisted over the ensuing 24 hours. The ability of the antioxidant TBAP to block BI 2536/vorinostat-mediated ROS generation and lethality indicates an important functional role for oxidative injury in synergistic interactions. While ROS generation could stem from DNA damage (41), the observation that TBAP blocked γH2A.X formation and ATM/ATR activation suggests that ROS generation operates upstream of DNA breaks.

In cells sustaining DNA damage, HDACIs perturb the G_1 checkpoint (42, 43), although interference with the intra-S (43) and G_2–M checkpoints (43) has also been described. Here, minimally toxic concentrations of vorinostat induced marked G_0–G_1 arrest, consistent with the ability of this agent to upregulate $p21^{CIP1}$ (32). Exposure to BI2536 or PLK1 knockdown produced modest but discernible G_2–M accumulation, reflecting the role of PLK1 in mitotic progression (44). Notably, vorinostat combined with BI2536 or PLK1 knockdown essentially abrogated G_0–G_1 arrest and resulted in a striking accumulation of cells in G_2–M phase. Thus, combining HDAC with PLK1 inhibition may disable the G_1 checkpoint while simultaneously increasing DNA damage, promoting accumulation of cells in G_2–M and subsequently apoptosis.

The combination of BI2536 and vorinostat showed marked inhibition of tumor growth of imatinib mesylate–sensitive or -resistant BCR/ABL^+ leukemias in both flank and systemic *in vivo* models and significantly increased survival compared with single agents. Notably, multiple events observed in cells exposed to these agents *in vitro* (e.g., BCR/ABL and STAT5 dephosphorylation, γH2A.X formation, and PARP cleavage occurred *in vivo*, suggesting that similar mechanisms may be operative in the latter setting. The relative lack of toxicity of this regimen was consistent with the minimal *in vitro* effects observed in normal hematopoietic cells ($CD34^+$). Transformed cells exhibit impaired DNA damage checkpoints (45) and increased PLK1 expression in leukemia (10) may reflect a compensatory mechanism designed to circumvent otherwise lethal effects of DNA damage. Thus, leukemia cells may be particularly vulnerable to a strategy combining PLK1 inhibition with HDACIs, which promote DNA injury while disrupting checkpoint mechanisms (46). Of note, the BI2536/vorinostat regimen displayed significant activity against large tumors in immunocompromised mice. Such tumors tend to be resistant to both conventional and targeted therapy as a consequence of impaired vasculature, a hypoxic environment, and a low growth fraction (47). The ability of the BI 2536/vorinostat regimen to induce substantial tumor regression in advanced disease argues that resistance resulting from these mechanisms may be circumvented, at least in part, by the current strategy.

HDACIs such as vorinostat are approved for the treatment of cutaneous T-cell lymphoma (CTCL; ref. 48). However, while a role for these agents in CML has not yet been established, recent studies suggest that HDACIs may interact with tyrosine kinase inhibitors to target CML stem cells (49). In light of preclinical evidence of activity of PLK1 inhibitors in CML (13) and early preclinical indications of *in vivo* activity of such agents in other diseases (e.g., non–Hodgkin lymphoma; ref. 50), the concept of enhancing PLK1 inhibitor activity with HDACIs warrants further attention. Accordingly, studies investigating PLK1/HDAC inhibitor interactions in

BCR/ABL-negative hematopoietic malignancies are currently underway.

Disclosure of Potential Conflicts of Interest

No potential conflicts of interest were disclosed.

Authors' Contributions

Conception and design: G. Dasmahapatra, S. Grant
Development of methodology: G. Dasmahapatra, S. Grant
Acquisition of data (provided animals, acquired and managed patients, provided facilities, etc.): G. Dasmahapatra, H. Patel, T.K. Nguyen, E. Attkisson, S. Grant
Analysis and interpretation of data (e.g., statistical analysis, biostatistics, computational analysis): G. Dasmahapatra, H. Patel, T.K. Nguyen, S. Grant
Writing, review, and/or revision of the manuscript: G. Dasmahapatra, S. Grant
Administrative, technical, or material support (i.e., reporting or organizing data, constructing databases): G. Dasmahapatra, T.K. Nguyen, E. Attkisson, S. Grant
Study supervision: G. Dasmahapatra, S. Grant

Grant Support

G. Dasmahapatra, H. Patel, and S. Grant were supported by awards CA63753, CA93738, and CA100866 from the NIH; award R6059-06 from the Leukemia and Lymphoma Society of America, the Multiple Myeloma Research Foundation, Myeloma Spore (P50CA142509), the V Foundation, and Lymphoma SPORE award 1P50 CA130805.

The costs of publication of this article were defrayed in part by the payment of page charges. This article must therefore be hereby marked *advertisement* in accordance with 18 U.S.C. Section 1734 solely to indicate this fact.

Received August 28, 2012; revised October 26, 2012; accepted November 18, 2012; published OnlineFirst November 30, 2012.

References

1. Druker BJ. Translation of the Philadelphia chromosome into therapy for CML. Blood 2008;112:4808–17.
2. Copland M, Hamilton A, Elrick LJ, Baird JW, Allan EK, Jordanides N, et al. Dasatinib (BMS-354825) targets an earlier progenitor population than imatinib in primary CML but does not eliminate the quiescent fraction. Blood 2006;107:4532–9.
3. Redaelli S, Piazza R, Rostagno R, Magistroni V, Perini P, Marega M, et al. Activity of bosutinib, dasatinib, and nilotinib against 18 imatinib-resistant BCR/ABL mutants. J Clin Oncol 2009;27:469–71.
4. Quintas-Cardama A, Kantarjian H, Cortes J. Imatinib and beyond–exploring the full potential of targeted therapy for CML. Nat Rev Clin Oncol 2009;6:535–43.
5. Neering SJ, Bushnell T, Sozer S, Ashton J, Rossi RM, Wang PY, et al. Leukemia stem cells in a genetically defined murine model of blast-crisis CML. Blood 2007;110:2578–85.
6. Archambault V, Glover DM. Polo-like kinases: conservation and divergence in their functions and regulation. Nat Rev Mol Cell Biol 2009;10:265–75.
7. Lapenna S, Giordano A. Cell cycle kinases as therapeutic targets for cancer. Nat Rev Drug Discov 2009;8:547–66.
8. Takaki T, Trenz K, Costanzo V, Petronczki M. Polo-like kinase 1 reaches beyond mitosis–cytokinesis, DNA damage response, and development. Curr Opin Cell Biol 2008;20:650–60.
9. Liu XS, Song B, Liu X. The substrates of Plk1, beyond the functions in mitosis. Protein Cell 2010;1:999–1010.
10. Renner AG, Dos SC, Recher C, Bailly C, Creancier L, Kruczynski A, et al. Polo-like kinase 1 is overexpressed in acute myeloid leukemia and its inhibition preferentially targets the proliferation of leukemic cells. Blood 2009;114:659–62.
11. Liu L, Zhang M, Zou P. Expression of PLK1 and survivin in diffuse large B-cell lymphoma. Leuk Lymphoma 2007;48:2179–83.
12. Steegmaier M, Hoffmann M, Baum A, Lenart P, Petronczki M, Krssak M, et al. BI 2536, a potent and selective inhibitor of polo-like kinase 1, inhibits tumor growth *in vivo*. Curr Biol 2007;17:316–22.
13. Gleixner KV, Ferenc V, Peter B, Gruze A, Meyer RA, Hadzijusufovic E, et al. Polo-like kinase 1 (Plk1) as a novel drug target in chronic myeloid leukemia: overriding imatinib resistance with the Plk1 inhibitor BI 2536. Cancer Res 2010;70:1513–23.
14. Rudolph D, Steegmaier M, Hoffmann M, Grauert M, Baum A, Quant J, et al. BI 6727, a Polo-like kinase inhibitor with improved pharmacokinetic profile and broad antitumor activity. Clin Cancer Res 2009;15:3094–102.
15. Bolden JE, Peart MJ, Johnstone RW. Anticancer activities of histone deacetylase inhibitors. Nat Rev Drug Discov 2006;5:769–84.
16. Glozak MA, Sengupta N, Zhang X, Seto E. Acetylation and deacetylation of non-histone proteins. Gene 2005;363:15–23.
17. Lee JH, Choy ML, Ngo L, Foster SS, Marks PA. Histone deacetylase inhibitor induces DNA damage, which normal but not transformed cells can repair. Proc Natl Acad Sci U S A 2010;107:14639–44.
18. Gao N, Rahmani M, Dent P, Grant S. 2-Methoxyestradiol-induced apoptosis in human leukemia cells proceeds through a reactive oxygen species and Akt-dependent process. Oncogene 2005;24:3797–809.
19. Ungerstedt JS, Sowa Y, Xu WS, Shao Y, Dokmanovic M, Perez G, et al. Role of thioredoxin in the response of normal and transformed cells to histone deacetylase inhibitors. Proc Natl Acad Sci U S A 2005;102:673–8.
20. Yu C, Rahmani M, Almenara J, Subler M, Krystal G, Conrad D, et al. Histone deacetylase inhibitors promote STI571-mediated apoptosis in STI571-sensitive and -resistant Bcr/Abl +human myeloid leukemia cells. Cancer Res 2003;63:2118–26.
21. Zhang B, Strauss AC, Chu S, Li M, Ho Y, Shiang KD, et al. Effective targeting of quiescent chronic myelogenous leukemia stem cells by histone deacetylase inhibitors in combination with imatinib mesylate. Cancer Cell 2010;17:427–42.
22. Dasmahapatra G, Yerram N, Dai Y, Dent P, Grant S. Synergistic interactions between vorinostat and sorafenib in chronic myelogenous leukemia cells involve Mcl-1 and p21CIP1 down-regulation. Clin Cancer Res 2007;13:4280–90.
23. Nguyen T, Dai Y, Attkisson E, Kramer L, Jordan N, Nguyen N, et al. HDAC inhibitors potentiate the activity of the BCR/ABL kinase inhibitor KW-2449 in imatinib-sensitive or -resistant BCR/ABL+ leukemia cells *in vitro* and *in vivo*. Clin Cancer Res 2011;17:3219–32.
24. Dasmahapatra G, Lembersky D, Kramer L, Fisher RI, Friedberg J, Dent P, et al. The pan-HDAC inhibitor vorinostat potentiates the activity of the proteasome inhibitor carfilzomib in human DLBCL cells *in vitro* and *in vivo*. Blood 2010;115:4478–87.
25. Dasmahapatra G, Lembersky D, Son MP, Attkisson E, Dent P, Fisher RI, et al. Carfilzomib interacts synergistically with histone deacetylase inhibitors in mantle cell lymphoma cells *in vitro* and *in vivo*. Mol Cancer Ther 2011;10:1686–97.
26. Chou TC, Talalay P. Quantitative analysis of dose-effect relationships: the combined effects of multiple drugs or enzyme inhibitors. Adv Enzyme Regul 1984;22:27–55.
27. Shuai K, Halpern J, ten HJ, Rao X, Sawyers CL. Constitutive activation of STAT5 by the BCR-ABL oncogene in chronic myelogenous leukemia. Oncogene 1996;13:247–54.
28. Konishi A, Shimizu S, Hirota J, Takao T, Fan Y, Matsuoka Y, et al. Involvement of histone H1.2 in apoptosis induced by DNA double-strand breaks. Cell 2003;114:673–88.
29. Celeste A, Petersen S, Romanienko PJ, Fernandez-Capetillo O, Chen HT, Sedelnikova OA, et al. Genomic instability in mice lacking histone H2AX. Science 2002;296:922–7.
30. Petruccelli LA, Dupere-Richer D, Pettersson F, Retrouvey H, Skoulikas S, Miller WH Jr. Vorinostat induces reactive oxygen species and DNA damage in acute myeloid leukemia cells. PLoS One 2011;6:e20987.
31. Bhaskara S, Knutson SK, Jiang G, Chandrasekharan MB, Wilson AJ, Zheng S, et al. Hdac3 is essential for the maintenance of chromatin structure and genome stability. Cancer Cell 2010;18:436–47.

32. Gui CY, Ngo L, Xu WS, Richon VM, Marks PA. Histone deacetylase (HDAC) inhibitor activation of p21WAF1 involves changes in promoter-associated proteins, including HDAC1. Proc Natl Acad Sci U S A 2004;101:1241–6.
33. Marks PA. The mechanism of the anti-tumor activity of the histone deacetylase inhibitor, suberoylanilide hydroxamic acid (SAHA). Cell Cycle 2004;3:534–5.
34. Fiskus W, Pranpat M, Balasis M, Bali P, Estrella V, Kumaraswamy S, et al. Cotreatment with vorinostat (suberoylanilide hydroxamic acid) enhances activity of dasatinib (BMS-354825) against imatinib mesylate-sensitive or imatinib mesylate-resistant chronic myelogenous leukemia cells. Clin Cancer Res 2006;12:5869–78.
35. Nimmanapalli R, Fuino L, Bali P, Gasparetto M, Glozak M, Tao J, et al. Histone deacetylase inhibitor LAQ824 both lowers expression and promotes proteasomal degradation of Bcr-Abl and induces apoptosis of imatinib mesylate-sensitive or -refractory chronic myelogenous leukemia-blast crisis cells. Cancer Res 2003;63:5126–35.
36. van de Weerdt BC, van Vugt MA, Lindon C, Kauw JJ, Rozendaal MJ, Klompmaker R, et al. Uncoupling anaphase-promoting complex/cyclosome activity from spindle assembly checkpoint control by deregulating polo-like kinase 1. Mol Cell Biol 2005;25:2031–44.
37. Subramanian C, Opipari AW Jr, Bian X, Castle VP, Kwok RP. Ku70 acetylation mediates neuroblastoma cell death induced by histone deacetylase inhibitors. Proc Natl Acad Sci U S A 2005;102:4842–7.
38. Smits VA, Klompmaker R, Arnaud L, Rijksen G, Nigg EA, Medema RH. Polo-like kinase-1 is a target of the DNA damage checkpoint. Nat Cell Biol 2000;2:672–6.
39. Reinhardt HC, Yaffe MB. Kinases that control the cell cycle in response to DNA damage: Chk1, Chk2, and MK2. Curr Opin Cell Biol 2009;21:245–55.
40. Smart DK, Ortiz KL, Mattson D, Bradbury CM, Bisht KS, Sieck LK, et al. Thioredoxin reductase as a potential molecular target for anticancer agents that induce oxidative stress. Cancer Res 2004;64:6716–24.
41. Zhan H, Suzuki T, Aizawa K, Miyagawa K, Nagai R. Ataxia telangiectasia mutated (ATM)-mediated DNA damage response in oxidative stress-induced vascular endothelial cell senescence. J Biol Chem 2010;285:29662–70.
42. Sambucetti LC, Fischer DD, Zabludoff S, Kwon PO, Chamberlin H, Trogani N, et al. Histone deacetylase inhibition selectively alters the activity and expression of cell cycle proteins leading to specific chromatin acetylation and antiproliferative effects. J Biol Chem 1999;274:34940–7.
43. Robert T, Vanoli F, Chiolo I, Shubassi G, Bernstein KA, Rothstein R, et al. HDACs link the DNA damage response, processing of double-strand breaks and autophagy. Nature 2011;471:74–9.
44. Vazquez-Martin A, Oliveras-Ferraros C, Cufi S, Menendez JA. Polo-like kinase 1 regulates activation of AMP-activated protein kinase (AMPK) at the mitotic apparatus. Cell Cycle 2011;10:1295–302.
45. Kastan MB, Bartek J. Cell-cycle checkpoints and cancer. Nature 2004;432:316–23.
46. Warrener R, Beamish H, Burgess A, Waterhouse NJ, Giles N, Fairlie D, et al. Tumor cell-selective cytotoxicity by targeting cell cycle checkpoints. FASEB J 2003;17:1550–2.
47. Maity A, Bernhard EJ. Modulating tumor vasculature through signaling inhibition to improve cytotoxic therapy. Cancer Res 2010;70:2141–5.
48. Grant S, Easley C, Kirkpatrick P. Vorinostat. Nat Rev Drug Discov 2007;6:1–2.
49. Li L, Wang L, Li L, Wang Z, Ho Y, McDonald T, et al. Activation of p53 by SIRT1 inhibition enhances elimination of CML leukemia stem cells in combination with imatinib. Cancer Cell 2012;21:266–81.
50. Shi J, Lasky K, Shinde V, Stringer B, Qian MG, Liao D, et al. MLN0905, a small molecule PLK1 inhibitor, induces anti-tumor responses in human models of diffuse large B-cell lymphoma. Mol Cancer Ther 2012;11:2045–53.